# Analysis of Density Distribution for Unsteady Butane Flow Using Three-Dimensional Digital Speckle Tomography

**Han Seo Ko***
*School of Mechanical Engineering, Sungkyunkwan University,*
*300 Chunchun-dong, Jangan-gu, Suwon, Kyunggi-do 440-746, Korea*
**Kwang-Hee Park, Yong-Jae Kim**
*Graduate School, Department of Mechanical Engineering, Sungkyunkwan University,*
*300 Chunchun-dong, Jangan-gu, Suwon, Kyunggi-do 440-746, Korea*

Transient and asymmetric density distributions have been investigated by three-dimensional digital speckle tomography. Multiple CCD images captured movements of speckles in three angles of view simultaneously because the flows were asymmetric and transient. The speckle movements between no flow and downward butane flow from a circular half opening have been calculated by a cross-correlation tracking method so that those distances can be transferred to deflection angles of laser rays for density gradients. The three-dimensional density fields have been reconstructed from the deflection angles by a real-time multiplicative algebraic reconstruction technique (MART).

**Key Words :** Digital Speckle Tomography, Butane Flow, Multiplicative Algebraic Reconstruction Technique (MART), Cross-Correlation

## Nomenclature

$b$ : Basis function
$C$ : Multiplicative correction vector
$f$ : Actual field
$\hat{f}$ : Guessed or intermediate objective function to be optimized
$\bar{f}$ : Average value of phantom field $f$
$G$ : Gladstone-Dale constant
$J$ : Equally spaced points in $x$ direction
$K$ : Equally spaced points in $y$ direction
$L$ : Equally spaced points in $z$ direction
$l$ : Distance between the test section and the viewing screen
$O_j$ : Height coefficient of $j$-th basis function
$Q$ : Flow rate
$q$ : Iteration number
$s$ : Coordinate on the projection plane, perpendicular to the ray direction
$t$ : Coordinate parallel to the ray direction
$W$ : Projection matrix
$W_{ij}$ : Weighting factor of MART
$w_i$ : $i$-th row of projection matrix
$(x, y, z)$ : Objective field coordinate
$Z$ : Maximum value of the computer-synthesized phantom field

### Greek Symbols

$\alpha$ : Line-of-sight beam deflection angle
$\delta$ : Speckle displacement
$\Phi$ : Reconstruction error
$\lambda$ : Laser wave length
$\theta$ : Angle of projection
$\rho$ : Density
$\psi$ : Measured projection
$\hat{\psi}$ : Virtual projection of guessed field

### Subscripts

$abs$ : Normalized absolute
$avg$ : Average
$IF$ : Interferometry

* Corresponding Author,
**E-mail** : hanseoko@yurim.skku.ac.kr
**TEL** : +82-31-290-7453; **FAX** : +82-31-290-5849
School of Mechanical Engineering, Sungkyunkwan University, 300 Chunchun-dong, Jangan-gu, Suwon, Kyunggi-do 440-746, Korea. (Manuscript **Received** November 15, 2003; **Revised** April 23, 2004)

*ref* : Reference condition
*rms*: Normalized rms
*SP* : Digital specklegram

## 1. Introduction

Laser speckle tomography measures density or temperature distributions using deflection angles from variation of refractive index of a phase object (Qui et al., 2001). The nonintrusive technique has a good resolution and can be applied for analysis of various thermal flows. The beam deflection angle $\alpha$ can be obtained from a ray integral of the field density gradient normal to the direction of the incident laser beam with the Gladstone-Dale constant $G$ (Partington, 1953):

$$\psi_{SP}(s,\ \theta) \cong \alpha = G\int \frac{\partial \rho}{\partial s}\, dt \qquad (1)$$

where $\psi_{SP}$ is the projection of the digital speckle system, $\alpha$ is the deflection angle, $\rho$ is the field density, $s$ is perpendicular to, and $t$ is parallel to the incident ray.

The tomography methods such as the algebraic reconstruction technique (ART) (Gordon, 1974) and multiplicative algebraic reconstruction technique (MART) (Verhoeven, 1993) update the density distributions by using the straightforward feedback information of the density itself instead of the density gradient. Thus, the ray deflection angle $\psi_{SP}$ from the digital speckle system should be converted to the interferometric fringe shift $\psi_{IF}$ which can be expressed as the integration of the density itself as follows:

$$\psi_{IF} = \frac{G}{\lambda}\int (\rho - \rho_{ref})\, dt \qquad (2)$$

where $\lambda$ denotes the wave length of laser ray. The interferometric fringe shift $\psi_{IF}$ can be calculated from the integral of the ray deflection $\psi_{SP}$ along s for the tomography method as follows:

$$\psi_{IF} = \frac{1}{\lambda}\int \psi_{SP} dS \qquad (3)$$

The objective of this study is to reconstruct the transient and asymmetric density distributions for downward butane flow using the three-dimensional digital speckle tomography from the simultaneous and instantaneous speckle-displacement measurements by the cross-correlation method. Thus, the specklegram images have been captured by three CCD cameras and an image capturing board simultaneously for three projection angles of view before the reconstruction as shown in Fig. 1.

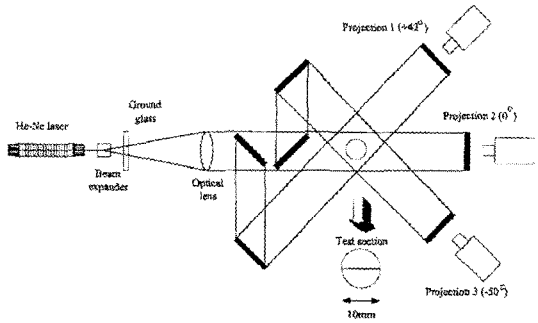


**Fig. 1** Schematic diagram of digital speckle system for downward butane flow

## 2. Digital Speckle Analysis

The digital speckle method just records the original speckle image and the dislocated speckle images separately using three CCD cameras as shown by Figs. 2(a) to (d) for downward butane flow. Then, the speckle movements are calculated by the cross-correlation method (Raffel et al., 1998) like a particle tracking method of a particle image velocimetry (PIV) (Kim, 2001). For the cross-correlation method, rectangular interrogation areas have been developed instead of square ones because most of the speckles in this study move horizontally as shown in Figs. 3(a) to (c) for the downward butane flow in three projection angles of view. There is no speckle outside the beam area and the nozzle position in Fig. 3. Thus, the cross-correlation has been performed by the random points, and the random arrows appeared in the areas, which can be negligible in Fig. 3. The speckle movements caused by the beam deflection angle are expressed as the arrows to identify the directions while the dots indicate no speckle displacement in Fig. 3. From the simultaneous and instantaneous measurements of the speckle dislocations using three projection angles

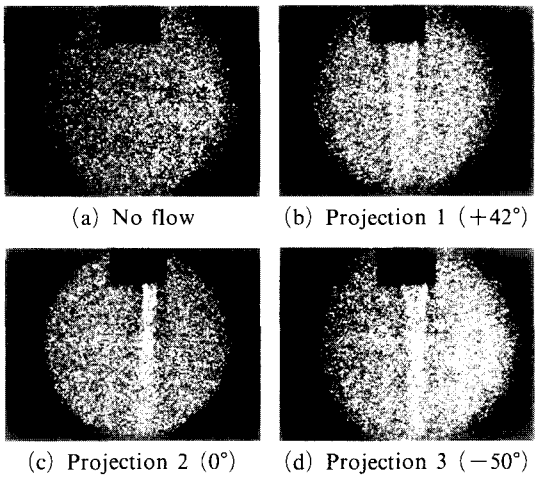

(a) No flow (b) Projection 1 (+42°)

(c) Projection 2 (0°) (d) Projection 3 (−50°)

**Fig. 2** Digital speckle images of downward butane flow for three projection angles of view ($Q$= 0.33 l/min)

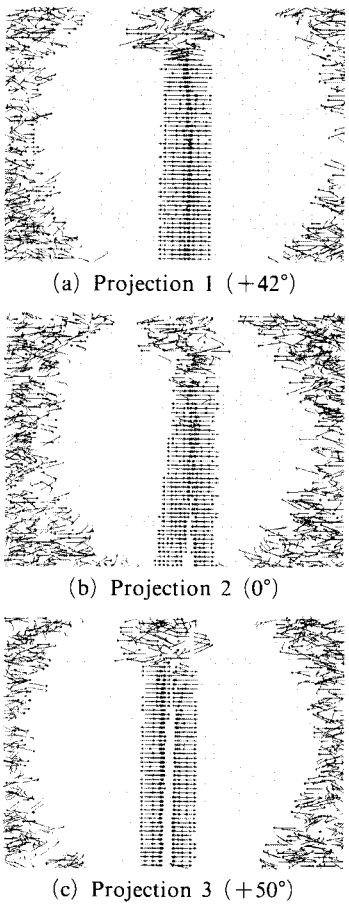

(a) Projection 1 (+42°)

(b) Projection 2 (0°)

(c) Projection 3 (+50°)

**Fig. 3** Speckle displacements by cross-correlation method for downward butane flow

of view, the deflection angles can be calculated as follows:

$$\alpha \cong \tan \alpha = \frac{\delta}{l} \tag{4}$$

where $\delta$ is the speckle displacements and $l$ is the distance between a test section and a viewing screen. The transient and asymmetric density distributions can be reconstructed by the tomography method after the deflection angle $\psi_{SP}$ is converted to the interferometric fringe shift $\psi_{IF}$ by Eq. (3).

## 3. Tomographic Reconstruction Algorithm : Multiplicative Algebraic Reconstruction Technique (MART)

The deflection angle, $\alpha$ in Eq. (1) must be inverted to reconstruct the true density field, $\rho(x, y, z)$ and this inversion procedure is called speckle tomography (Fomin, 1998). The tomography undertakes the optimization task for the linear case where each basis function is defined by a single parameter (usually its unknown height with a fixed spread). The location of each basis function is given as

$$\hat{f}(x, y, z) = \sum_{j=1}^{JKL} O_j b(x - x_j, y - y_j, z - z_j) \tag{5}$$

where $\hat{f}$ is an object function that represents the field to be reconstructed, $b$ is a general form of the basis function located at $(x_j, y_j, z_j)$, and $O_j$ is the height coefficient of the $j$-th basis function centered at a fixed location of $(x_j, y_j, z_j)$. The $(x_j, y_j, z_j)$ positions form a rectangular array of $J$, $K$ and $L$ equally spaced points in the $x$, $y$ and $z$ directions, respectively. Thus, $J \times K \times L$ is the total number of coefficients to be estimated by the reconstruction algorithm. The use of a smooth basis function such as the cubic B-spline function (Hanson and Wecksung, 1985) can accurately represent a relatively smooth object field with far fewer coefficients (unknowns) than with the square-pixel basis function. An optimized set of these unknowns must be found to minimize the deviations between the virtual projection $\hat{\psi}$ of an intermediate object function $\hat{f}$ and the

measured projection $\psi$ of the actual field $f$. The developed three-dimensional tomography in this study reconstructs the three-dimensional density field simultaneously instead of piling up the cross-sectional density distributions because the three-dimensional objection function has been expressed by Eq. (5), which is an originality of this study as compared with previous two-dimensional reconstructions.

The multiplicative algebraic reconstruction technique (MART) uses an element $C_j$ of the multiplicative correction vector $C$ as follows:

$$Q_j^{q+1}=C_j^q Q_j^q$$

$$C_j^q=\begin{cases}1-0.5\,W_{i,j}\left(1-\dfrac{\psi_i}{\hat{\psi}_i}\right), & \hat{\psi}_i\neq 0\\ 1 & \text{otherwise}\end{cases} \tag{6}$$

where $q$ denotes the $q$-th iteration and the normalized weighting factor $W_{i,j}$ is equal to $w_{i,j}/w_{\max}$ where $w_{\max}$ is the largest element of the projection matrix $W$. One advantage of using MART is to ensure a non-negative object field in reconstructing non-negative scalar.

Note that the algorithm update, in principle, is possible only for algebraic projections in which the ray integration of the field directly gives the projection data, such as in interferometry (Eq. (2)). Therefore, for the digital specklegram the ray sum must be changed from $\psi_{SP}$ to $\psi_{IF}$ by Eq. (3) and the three-dimensional MART can be used to calculate the three-dimensional density distributions simultaneously. Although the digital speckle analysis requires one more step for integrating the deflection angles to calculate the fringe shifts, the results of the digital specklegram give a smooth density distribution and acceptable accuracy as compared with those of the Mach-Zehnder interferometry because lots of the speckles are used to measure the deflection angles for the tomography.

## 4. Numerical Analysis

The accuracy of the three-dimensional tomography has been investigated before the experiment using a three-dimensional computer-synthesized phantom field which is modified from the cosine phantom (Verhoeven, 1993) as follows:

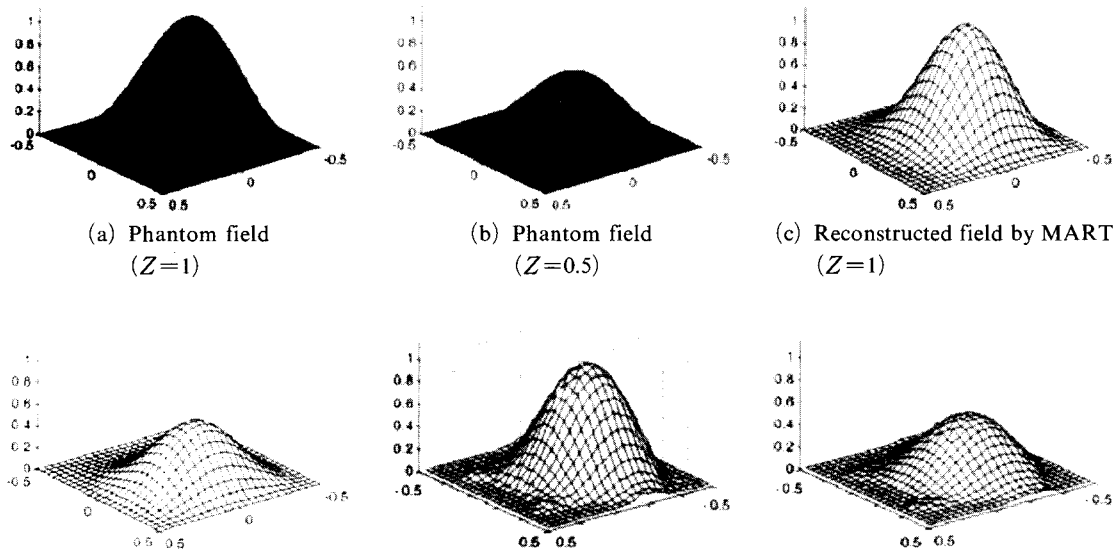

(a) Phantom field ($Z=1$) (b) Phantom field ($Z=0.5$) (c) Reconstructed field by MART ($Z=1$)

(d) Reconstructed field by MART ($Z=0.5$) (e) Reconstructed field by ART ($Z=1$) (f) Reconstructed field by ART ($Z=0.5$)

**Fig. 4** Comparison of reconstructed fields with phantom fields by MART and ART

$$f(x, y, z) = \begin{cases} \dfrac{[1-\cos\{2\pi(x+0.5)\}][1-\cos\{2\pi(y+0.5)^{3/2}\}](1-z)}{4}, & |x, y|<0.5, |z|<1 \\ 0 & \text{otherwise} \end{cases} \quad (7)$$

The projection data have been calculated from Eq. (7) and then the three-dimensional ART (Ko and Kim, 2002) and the MART have been performed numerically to confirm the accuracies.

For the case of the three-dimensional reconstruction, more numbers of the projection data are required to calculate accurately than those of the two-dimensional reconstruction. The total number of rays for this three-dimensional reconstruction was 5400 including three equal-spaced projection angles (+45°, 0°, −45°) in one plane, 18 planes in $z$-direction, and 100 rays in each projection angle ($3\times18\times100=5400$). Acceptable accuracies have been confirmed by the ART and the MART as shown by Fig. 4. The calculated results of the three-dimensional MART show better reconstructions than those of the ART (Fig. 4).

Three different error measurements are used in this research. The first is the average error of the reconstructed object function $\hat{f}$ and the reference phantom function $f$ (Ko and Kim, 2002):

$$\Phi_{avg} = \frac{\sum_{j=1}^{JKL} |f(x_j, y_j, z_j) - \hat{f}(x_j, y_j, z_j)|}{JKL} \quad (8)$$

where $JKL$ is the total number of the basis functions used to conform to the reconstructing object functions. The second is a normalized rms error:

$$\Phi_{rms} = \sqrt{\frac{\sum_{j=1}^{JKL} [f(x_j, y_j, z_j) - \hat{f}(x_j, y_j, z_j)]^2}{\sum_{j=1}^{JKL} [f(x_j, y_j, z_j) - \bar{f}]^2}} \quad (9)$$

where $\bar{f}$ is the average value of the phantom field $f$. The normalized rms error is large if there are a few large errors in the reconstruction. The third one is a normalized absolute error:

$$\Phi_{abs} = \frac{\sum_{j=1}^{JKL} |f(x_j, y_j, z_j) - \hat{f}(x_j, y_j, z_j)|}{\sum_{j=1}^{JKL} |f(x_j, y_j, z_j)|} \quad (10)$$

which emphasizes the effect of many small errors. Note that these three errors measure the reconstruction quality based on the comparison between the reconstructed field (object function) and the true field (phantom function) (Liu et al., 1989). However, the true field is unknown in a real experiment and the quality of reconstruction is only measured by comparing the virtual projection $\hat{\psi}$ against the measured projection $\psi$.

The errors have been calculated and compared using Eqs. (8), (9) and (10) as shown by Table 1. As the number of the iteration increases, the error values decrease for higher accuracies. Also, the MART shows better reconstructions than the ART does. Thus, the MART has been used to reconstruct the three-dimensional density field for the experimental data. Since the accuracies do not improve with infinite numbers of the iteration, the number of iterations for the minimum error can be pointed out to stop the itera-

**Table 1** Comparison of reconstruction errors between ART and MART methods for three-dimensional density distributions

| Iteration | Tomography Method | $\Phi_{avg}$(%) | $\Phi_{rms}$(%) | $\Phi_{abs}$(%) |
|---|---|---|---|---|
| 100 | ART | 1.05 | 1.08 | 10.4 |
| | MART | 0.79 | 0.64 | 7.82 |
| 1000 | ART | 0.97 | 0.95 | 9.67 |
| | MART | 0.74 | 0.54 | 7.36 |

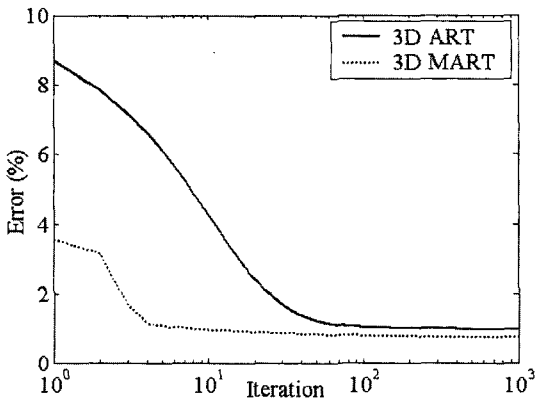


**Fig. 5** Average error versus iteration for reconstruction of computer-synthesized phantoms

tion step and reconstruct the field at that point (Fig. 5). If the shape of the reconstructed field is complex, the number of the iteration for the acceptable accuracy increases.

## 5. Experimental Setup

The downward butane flow from the half-blocked circular nozzle has been measured by a 35 mW He-Ne laser using the three-dimensional digital speckle tomography. The nozzle is made of copper and the inside diameter is 10 mm. The laser beam is expanded by a 5×beam expander and directed at an optical lens via a ground glass as shown by Fig. 1.

After opening the valve for the downward butane flow perpendicular to the laser beam, the valve has been closed to capture the images of the reducing butane flow for 3 seconds by three CCD cameras. For the experiment, the specklegram images have been captured by three CCDs in three different angles of view simultaneously because the measured butane flow is asymmetric and unsteady. From those three specklegram images, the speckle movements have been calculated by the cross-correlation method. And then, the three-dimensional and transient density distributions have been reconstructed by the developed real-time and three-dimensional MART in this study.

## 6. Results and Discussion

The three-dimensional density distribution has been reconstructed from 11 mm to 21 mm below the nozzle after calculating the speckle movements by the cross-correlation method. The performed three-dimensional MART has used three projection angles of view in one plane (+42°, 0°, −50°), 18 planes in $z$-direction, and 100 rays in each projection angle. Because of the space limitation, the intervals (+42° and −50°) of the projection angle were not perfectly equivalent. Although the three-dimensional reconstruction has been carried out for all of the heights in $z$-direction simultaneously, Figure 6 shows the reconstructed density fields from 11, 16 and 21 mm below the nozzle with the time interval of 1 second because of the page limitation.

The peak values of the butane densities are close to 100% of pure butane density (2.4 kg/m$^3$) for 1 second after closing the valve as shown in Figs. 6(a), (b) and (c). Also, the noises do not appear much in those figures because the mixture of air and butane is relatively low. Since the tomography has been carried out using three projection angles, the small error can occur near the measuring part. If the number of view increases, the noise can be reduced.

As the time passes, the flow rate of the butane decreases and the mixture with air increases. Thus, the absolute value of the butane density reduces and the more noise appear as shown by Figs. 6(d), (e) and (f). For the case of 3 seconds after closing the valve, the noises become relatively higher because the butane flow is mixed more with air and affected by the surrounding air flow sensitively as shown in Figs. 6(g), (h) and (i).

The butane density varies not only by the time change but also by the height change. Thus, the butane densities for 16 mm below the nozzle (Figs. 6(b), (e) and (h)) are lower than those for 11 mm from the nozzle (Figs. 6(a), (d) and (g)) because of more mixture with the air by the distance from the nozzle end. However, the densities for 21 mm below the nozzle (Figs. 6(c), (f) and (i)) do not show big discrepancies with those for 16 mm below the nozzle because the distance from the nozzle and the effect of the noises are already large for those relatively low densities.

The calculation of the tomography has been performed in IBM PC with the P4-2. 0 GHz and the RAM of 1 Gbyte and the average number of the iteration was 3 for the average calculation time of 5 minutes 12 seconds. If the number of the iteration increases more than 3, the profile of the density distribution includes more noises. Thus, the iteration has been stopped at the point for the accurate reconstruction. The developed digital speckle tomography can be used for the simultaneous three-dimensional density reconstructions of various gas flows in order to detect the real-time gas leakage.

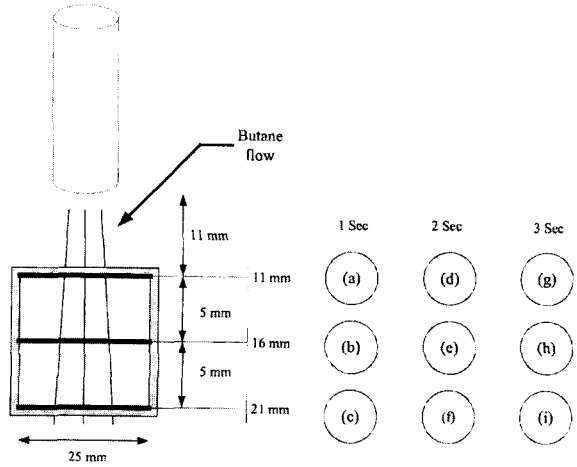


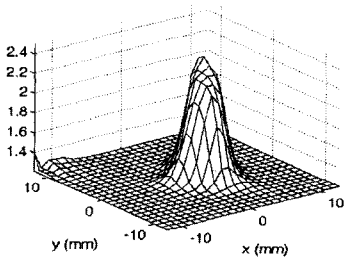


(a) 11 mm from nozzle for 1 sec after closing

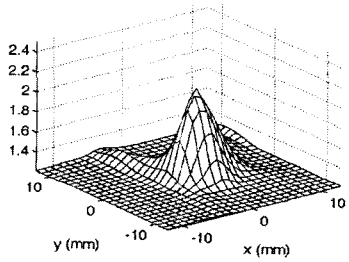


(b) 16 mm from nozzle for 1 sec after closing

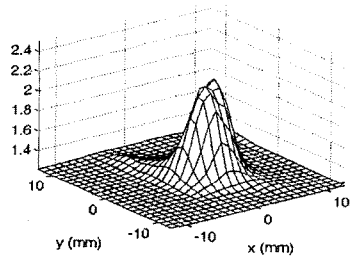


(c) 21 mm from nozzle for 1 sec after closing

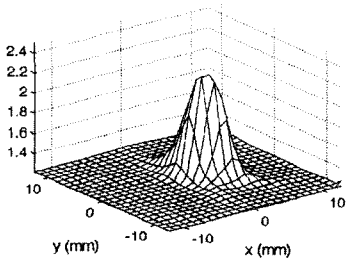


(d) 11 mm from nozzle for 2 sec after closing

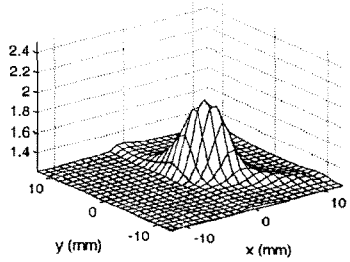


(e) 16 mm from nozzle for 2 sec after closing

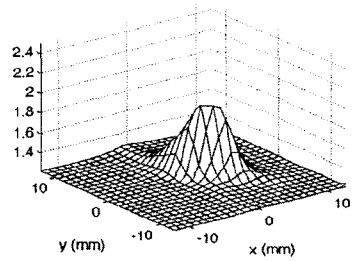


(f) 21 mm from nozzle for 2 sec after closing

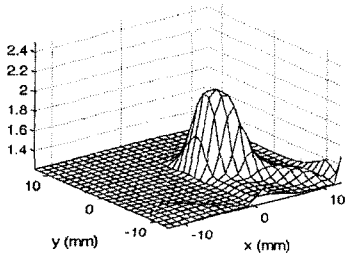


(g) 11 mm from nozzle for 3 sec after closing

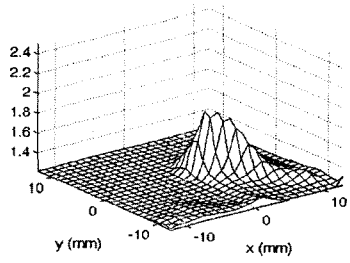


(h) 16 mm from nozzle for 3 sec after closing

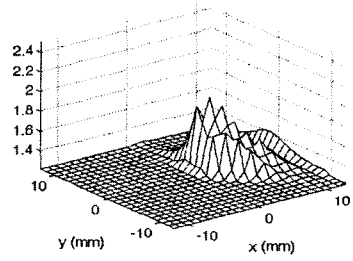


(i) 21 mm from nozzle for 3 sec after closing

**Fig. 6** Reconstructed three-dimensional density distributions of transient butane flow from half-blocked nozzle

## 7. Concluding Remarks

The three-dimensional density distribution has been reconstructed using the developed real-time digital speckle tomography in this study. The noises for the tomography appeared more as the distance between the reconstructed density field and the nozzle increased and the flow rate decreased because of the mixture with air. Also, the numerical error was found because the three projection angles of view were used to perform the tomography. In the experiment, the noises could be caused by the small vibration of the camera and the unstable surrounding air. The three-dimensional MART which has been confirmed in the numerical study has reconstructed the asymmetric and transient density distributions of the butane flow with acceptable accuracies. This study can be applied for the inspection of the gas leakage and the accurate analysis of various thermal flows.

## Acknowledgment

This work was supported by grant No. R08-2003-000-10030-0 from the Basic Research Program of the Korea Science & Engineering Foundation.

## References

Fomin, N. A., 1998, *Speckle Photography for Fluid Mechanics Measurements*, Springer, Berlin.

Françon, M., 1979, *Laser Speckle and Applications in Optics*, Academic Press, New York.

Gordon, R., 1974, "A Tutorial on ART," *IEEE Trans. on Nuclear Science*, Vol. NS~21, pp. 78~92.

Hanson, K. M. and Wecksung, G. W., 1985, "Local Basis Function Approach to Computed Tomography," *Appl. Opt.*, Vol. 24, No. 23, pp. 4028~4039.

Kak, A. C. and Slaney, M., 1987, *Principles of Computerized Tomographic Imaging*, IEEE Press, New York.

Kastell, D., Kihm, K. D. and Fletcher, L. S., 1992, "Study of Laminar Thermal Boundary Layers Occurring around the Leading Edge of a Vertical Isothermal Wall Using a Specklegram Technique," *Exper. Fluids*, Vol. 13, pp. 249~256.

Kihm, K. D., 1997, "Laser Speckle Photography Technique Applied for Heat and Mass Transfer Problems," *Advan. in Heat Transfer*, Vol. 30, pp. 255~311.

Kihm, K. D., Ko, H. S. and Lyons, D. P., 1998, "Tomographic Identification of Gas Bubbles in Two-Phase Flows with the Combined Use of the Algebraic Reconstruction Technique and the Genetic Algorithm," *Opt. Lett.*, Vol. 23, No. 9, pp. 658~660.

Kim, S. K., 2001, "An Experimental Study of Developing and Fully Developed Flows in a Wavy Channel by PIV," *KSME Int. J.*, Vol. 15, No. 12, pp. 1853~1859.

Ko, H. S., Ikeda, K. and Okamoto, K., 2002, "Combination of Holographic Interferometry and Digital Speckle System for Measurement of Density Distributions," *Meas. Sci. Tech.*, Vol. 13, No. 12, pp. 1974~1978.

Ko, H. S. and Kihm, K. D, 1999, "An Extended Algebraic Reconstruction Technique (ART) for Density-Gradient Projections : Laser Speckle Photographic Tomography," *Exper. Fluids*, Vol. 27, No. 6, pp. 542~550.

Ko, H. S. and Kim, Y. -J., 2002, "Comparison and Analysis of Tomography Methods for Reconstruction of Three-dimensional Density Distributions in Two-phase Flows," *J. Nondestructive Testing*, Vol. 22, No. 5, pp. 545~556.

Ko, H. S. and Kim, Y. -J., 2003, "Tomographic Reconstruction of Two-phase flows," *KSME Int. J.*, Vol. 17, No. 4, pp. 571~580.

Ko, H. S., Lyons, D. P., and Kihm, K. D., 1997, "A Comparative Study of Algebraic Reconstruction (ART) and Genetic Algorithms (GA) for Beam Deflection Tomography," *ASME Fluids Engrg. Div. Summer Meeting*, Vancouver, Canada, Paper FEDSM 97~3104.

Liu, T. C., Merzkirch, W., and Oberste-Lehn, K., 1989, "Optical Tomography Applied to a Speckle Photographic Measurement of Asymmetric Flows with Variable Density," *Exper. Fluids*, Vol. 7, pp. 157~163.

Partington, J. R., 1953, *Physico-Chemical Optics*, Vol. IV, An Advanced Treatise on Physical Chemistry, Longmans Green, London.

Qiu, H., Hsu, C. T. and Liu W., 2001, "The Effect of Second Order Refraction on Optical Bubble Sizing in Multiphase Flows," *KSME Int. J.*, Vol. 15, No. 12, pp. 1801~1807.

Raffel, M., Willert, C. E. and Kompenhans, J., 1998, *Particle Image Velocimetry*, Springer, Berlin.

Verhoeven, D., 1993, "Limited-data Computed Tomography Algorithms for the Physical Sciences," *Appl. Opt.*, Vol. 32, No. 20, pp. 3736~3754.